MULTILEVEL SELECTION IN MODELS OF PREBIOTIC EVOLUTION: COMPARTMENTS AND SPATIAL SELF-ORGANIZATION

PAULIEN HOGEWEG[1]* and NOBUTO TAKEUCHI[1,2]
[1] *Theoretical Biology and Bioinformatics Group, Utrecht University, Utrecht, The Netherlands;*
[2] *Biological Institute, Tohoku University, Sendai, Japan*
(author for correspondence, e-mail: p.hogeweg@bio.uu.nl)*

(Received 7 August 2002; accepted in revised form 11 October 2002)

Abstract. In this paper we explore the impact of new levels of selection in models of early evolution. We contrast two types of higher levels of selection. On the one hand we look at spatially explicit models of replicators in which, by a process of self-organization, new levels of selection arise as large scale spatial patterns with a dynamics of their own. Alternatively externally imposed levels of selection above the basic replicators are created by enclosing the replicators in vesicles. In this paper we first review some results on the impact of emerging higher levels of selection on the evolutionary persistence of interacting co-evolving replicator systems. Moreover, we present a vesicle model, which can potentially integrate emerging and imposed levels of selection. We use the models to examine the classical problem information integration in early evolution.

Keywords: cellular automata model, error threshold, hypercycle stochastic corrector model, information threshold simulation model, multilevel evolution

1. Introduction

Although there has been much discussion on what is the appropriate level on which Darwinian selection operates, we now know that in many cases the interesting features arise through the occurrence of multiple levels of selection which act in concordance and/or in conflict. Indeed, symbiogenesis of initially independently replicating entities underly major transitions in evolution leading to complex life forms (Maynard Smith and Szathmary, 1995). It appears not only that the formation of multiple levels of selection shaped living systems on this planet, models show that the occurrence of new levels of selection is an inevitable property of eco-evolutionary processes when interactions occur locally in space (e.g. Boerlijst and Hogeweg, 1991; Hogeweg, 2002).

Classical, single level, models of replicator dynamics have revealed a fundamental problem about information accumulation through a process of mutation and Darwinian selection, the so-called information threshold (Eigen *et al.*, 1989). Selection can counterbalance only a limited mutation rate, and therefore, assuming a certain rate of replication error per nucleotide, only a limited sequence length can be evolutionary maintained. A certain amount of information (sequence length)

Origins of Life and Evolution of the Biosphere **33:** 375–403, 2003.

should be needed in order to improve copying fidelity, and therefore the information threshold could be a major barrier in early evolution.

To overcome the information threshold two types of scenario's have been proposed: cooperative interactions and compartments. The hypercycle model is the classical example of the former and the stochastic corrector model that of the latter. The hypercycle model proposes a cyclic interaction structure of catalytic self-replicating molecules, and its dynamic properties have been extensively studied. Apart from biochemical considerations, a major problem of hypercycles as a means to overcome the information threshold is its sensitivity to so called 'parasites' whose replication is strongly catalyzed, but who do not catalyze the replication of any of the other molecules, and thereby break the cycle. This vulnerability to parasites is less severe in spatial models, in which multiple levels of selection operate and thus change the invasion dynamics of mutants dramatically. Nevertheless, as we will review below, the evolutionary instability of this interaction structure makes it an unattractive candidate for overcoming the information threshold. However, the emergence of higher levels of selection in spatial models widen the class of potential interaction structures which can persist enormously. We will review in Section 3 the longterm eco-evolutionary stability of several interaction structures, and show the potential feasibility in space for enhanced information integration due to cooperative interactions.

The stochastic corrector model also invokes higher levels of selection to overcome the dynamic trends of the lower level dynamics. However, these higher levels of selection are imposed rather than a result of the lower level dynamics. The evolving replicating molecules are assumed to be enclosed in vesicles, which themselves are subject to a Darwinian regime. The 'negative mutations' arise mainly from the dynamics of the molecules, the (relative) 'positive mutation', which 'correct' the evolutionary trends at the micro level, occur by stochastic fluctuations in the dynamics, and at vesicle division, in which molecules are randomly partitioned between the daughter cells. Potential problems of this scenario for overcoming the information threshold are that the 'stochastic corrector' mechanism works mainly for small compartment sizes, with small populations of the molecules, where stochastic effects are large, whereas the the information threshold shifts to lower mutation rates at small population sizes, and at small diffusivity.

In this paper we present a model which combines the potential for the emergence of new levels of selection through spatial pattern formation, with the inclusion of vesicles, which constitute a new level of selection above the molecular dynamics. We use the model to quantify the negative effects of both spatial pattern formation and of small compartment size on the information threshold, relative to the potential positive effects through compartmental dynamics. We show that also relatively large vesicles can benefit from the stochastic corrector mechanism, be it to a more limited extent than smaller vesicles in most regimes. However, in all cases studied the positive effect of the stochastic corrector mechanism is limited due to vesicle level dynamics.

2. Models and Methods

2.1. Replicator dynamics

We use replicator based, stochastic cellular automata models to describe the microscopic dynamics of evolutionary systems. A uniform grid of patches represents the space. The state of each patch represents the individual molecule, which inhabits that part of the space. This molecule can interact only with the molecules/space in its directs neighborhood, moves around locally, replicates and dies. Each individual may be unique, and calculate its interactions with its neighbors (in that case 'systolic array' is more accurate name than cellular automaton). The potential uniqueness of each individual is of course useful in evolutionary context. Therefore this type of models is not 'a poor mans choice' but actually should be preferred above e.g. partial differential equation models. The basic rules are:

(1) if a patch is empty neighboring individuals compete to put an offspring in it.
(2) this competition can be dependent on the interaction the neighbors have with their neighbors, e.g. whether they are being catalyzed.
(3) molecules decay with a certain probability.
(4) one or more diffusion steps occurs in between reaction steps.

2.2. Vesicle dynamics

We use the cell model proposed by Glazier and Graner (1993) to introduce vesicles in a CA layer on top of the spatial replicator dynamics defined above. This is a two scale CA model in which the cells/vesicles comprise many grid-cells. The dynamics of the vesicles is governed by the following energy minimization term:

$$H = \sum \frac{J_{ij}}{2} + \sum J_{im} + \sum \lambda (v - V)^2 \,,$$

where J_{ij} and J_{im} denote surface energy in between vesicles and with respect to the medium, respectively (here they are both 5), V is the target volume of the vesicle (here 100 for all vesicles) and v is its actual volume. In between each reaction step of the replicators, the vesicles adjust their boundary so as to minimize H as follows:
(1) each grid cell of the CA is considered in random order; iff the corresponding grid point in the replicator layer is empty (2) a neighboring grid point of the current point is randomly chosen; (3) the state (i.e. vesicle identification number) of the neighboring grid is copied into the current grid point with a probability of $p = 1$ if $\Delta H < D$ otherwise $p = \exp(-(\Delta H + D)/T)$. ΔH is the change in H if copying were to occur, D (=0.8) is the dissipation constant and T (=4) defines the randomness. In this way molecules remain in their own vesicles, and vesicles expand (contract) so as to attain the target size, but this expansion is constraint by the availability of space.

Vesicles divide under influence of the molecules which inhabit it. We use a simple threshold function on the number of (types of) molecules. Vesicle division is perpendicular to its longest axis, and the daughter vesicles simply inherit the molecules which are present in their half. The daughter vesicles try again to attain the target size. Expansion of the vesicles aids the replicator dynamics by creating space. Note that unlike previous models there is a mutual influence of molecules on vesicles and of vesicles on molecules. Note moreover that vesicles are localized in space, and pattern formation among the vesicles potentially forms a next level of selection above the vesicle level in a manner similar to that of pattern formation in the molecular dynamics. Figure 5 illustrates the model, as well as this clumping effect.

We apply the model to study whether and how much the information threshold defined by the molecular dynamics can be increased due to vesicle level selection⋆. We study various selection regimes on the vesicle level. All cases are such that the microscopic dynamics and the macroscopic dynamics act in concordance, i.e. what is 'good' for the molecules is 'good' for the vesicles. The regimes differ in whether and how the vesicles 'recognize' the types of molecules which inhabit them. We will show that only in the cases that the vesicles recognize the molecules and add extra selective advantages, the mutation rate at which the information threshold occurs is shifted to higher values.

3. Spatial Pattern Formation and the Eco-evolutionary Persistence of Catalyzed Replication

In this section we review work on the impact of higher levels of selection, which emerge automatically in spatial models of interacting replicators. This impact is profound in many models, reversing selection pressures, and enslaving the evolutionary fate of the micro level entities to the spatial-temporal patterns they create. This was first demonstrated in the context of the hypercycle model (Boerlijst and Hogeweg, 1991a, b).

These early studies were done as invasion experiments, i.e. after a stable spatio temporal attractor was reached the fate of an introduced mutant population was studied. Thus, a separation of time-scales was imposed between 'ecological dynamics' and 'evolutionary dynamics'. Indeed the original studies on hypercycles (Eigen and Schuster, 1979) considered only the ecological dynamics notwithstanding the fact that they were introduced as a potential solution for the information threshold problem, which arises due to high mutation rates. Similarly the stochastic corrector model was also studied in absence of mutations. In this paper we rectify this discrepancy by studying coupled eco-evolutionary dynamics.

⋆ 'Increase/decrease of the information threshold' is used as equivalent to 'increase/decrease of the critical mutation rate above which master sequences are not maintained in the system'.

In contrast to mean field models, in space not only cyclic interaction architectures are stable in ecological time, but also non-cyclic interaction structures, e.g. a self catalyzing replicator and its parasites (see e.g. Boerlijst and Hogeweg, 1991b; Hogeweg, 1994; Couwenberg, 1997; Czaran and Szathmary, 2000; McCaskill *et al.*, 2001; Fuchslin and McCaskill, 2001). In this section we compare several architectures with respect to their eco-evolutionary persistence. We study apart from the hypercycle model and the above mentioned minimal model of catalytic replicators and their parasites, a two membered hypercycle with its parasites, RNA-replicases, consisting of a plus and a minus string, of which e.g. the minus string is catalytic and their parasites, and finally duplex forming RNA's in which the minus strings of two populations can ligate and the duplex serves as replicase for these populations as well as other RNA's not participating in the duplex formation. Note that in mean field situation all these interaction structures are unstable, and die out very quickly. The CA rules are:

1. determine the catalysis each molecule gets. An interaction partner is chosen among the 8 neighbors proportional to the amount of catalysis they give; the received catalysis is stored;
2. an empty position chooses one of its 8 neighbors proportional to the catalysis they get, and receives its offspring; the offspring is either identical to the chosen neighbor (or in case of the RNA models its complement), or undergoes mutation; i.e. a new state is created with interactions to all other molecules slightly changed relative to those of the parent (in the RNA based model it involves creation of both a plus and a minus molecule) Occupied patches have a probability d = 0.15 of becoming empty;
3. one Margolus diffusion step (see Toffoli and Margolus, 1987);
4. iterate;
5. the default initial conditions are randomly distributed monotypic populations of the replicase(s) and the parasite(s), all in equal numbers. Parasites are initiated with 1.5 times the catalysis of the replicators. The CA has 200×200 cells, and zero boundary conditions;
6. mutation rates were varied from 0.0002 to 0.1024 in a geometric series.

We first study the eco-evolutionary properties of these interaction architectures by assuming that mutations only change the parameters of the interactions, but not the topology of the interaction network. Mutants inherit interaction parameters to all existing species from their parents with small perturbations, but do not create new interactions. We do, however, also study versions of the model in which interaction can be lost, to study the influence of perpetual parasite creation. Note that this 'interaction based' representation assumes that a mutation can change the interaction with many partners subtly and independently (e.g. by conformational changes). We checked the results in models where changes to all interaction partners were coordinated; this does not qualitatively change the results.

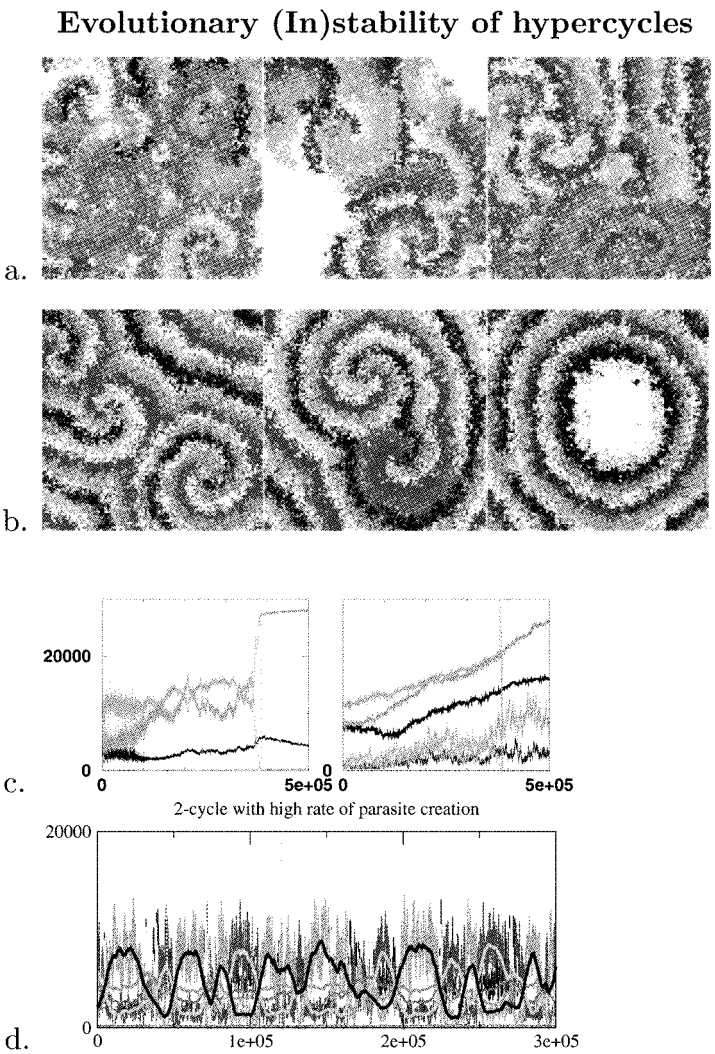

Figure 1. Upper panels (a, b): (in)stability of multi-membered hypercycles. Snapshots of the spatial distribution of the replicators of the hypercycle are shown. The colors indicate different genotypes and are chosen arbitrarily. White indicates empty space (i.e. local extinction). Panel (a): the system is initially able to expulse parasites in ecological time, although local extinction does occur. Panel (b): because of loss of number of spirals over time, it will become extinct due to breakup of the last spiral core. The breakup is caused by drift of catalysis strength (mutation rate = 0.0002) Lower panels (c, d): stability 2-membered hypercycle. 2 membered hypercycles can stably coexist with a parasite on one of the species over (long) ecological time, but the parasite in the end will be expelled due to the evolutionary dynamics. (c) Mutation rate = 0.0002; left panel: population size, color code: orange: parasite, brown: species 2, black: species 1 (which gives catalysis to parasite). Parasite dies out at ca. t = 400 000. Right panel upper lines increase of catalysis; lower lines population diversity (*3, for display purposes). Color coding as in population graph. (d) Evolutionary oscillations for continued influx of parasites on both members of the hypercycle. population numbers and running averages are shown. Strong oscillations are of the parasites, i.e. population averages in cyan and black. Mutation rate = 0.0512, parasite are created with 3 times more increase in catalysis than 'normal' mutants.

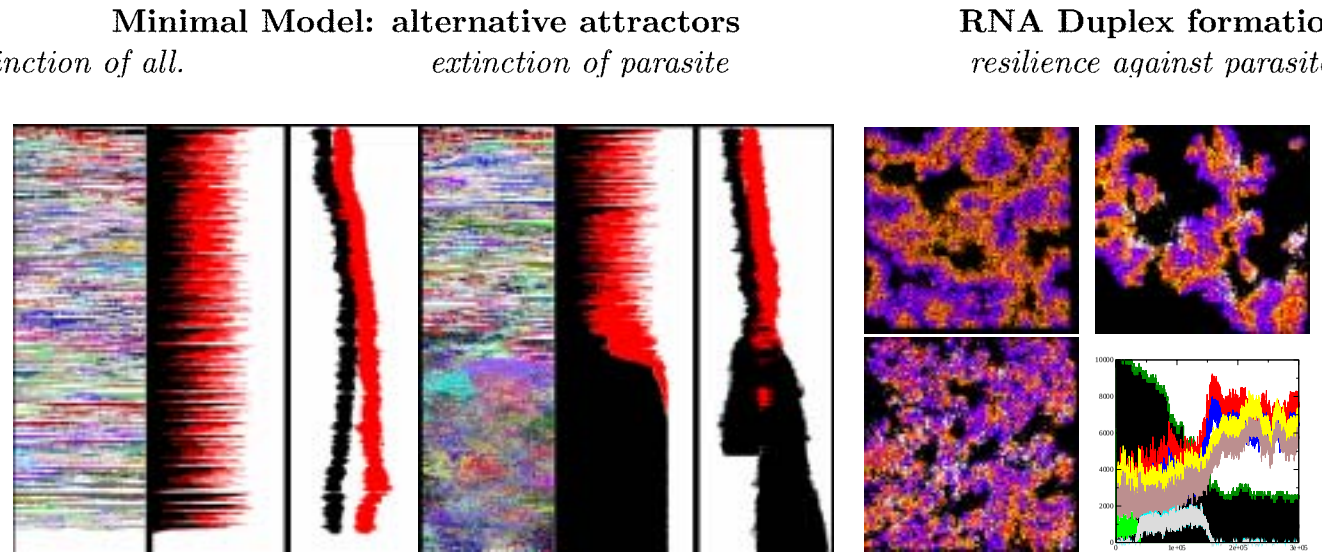

Figure 2. Minimal model. Mutation rate = 0.0032: left extinction, right parasite extinction, and catalysts diversification. In both cases we show (1) space time plot (colors indicate different genotypes), (2) population numbers (black catalysts, red parasite, all genotypes summed) and (3) catalysis strength (color as in (2)). Print interval 50 time steps. Duplex formation. Mutation rate = 0.0032, initial ligation probability = 0.50. Snapshots of spatial patterns. Color code: yellow and red, and blue and magenta are the plus and minus string of RNA-1 and RNA-2, respectively (genotypic variants within these categories not distinguished); white parasite plus and minus string; black empty space. Upper left without parasite. Upper right with parasite (white): ligation = 0.30. Lower left ligation probability fixed at 0.15. Lower right population sizes over time, mutation rate 0.004; initial ligation probability 0.50. Parasites are expelled because ligation probability evolves to low values. Black shaded area indicates maximum ligation strength in population (*200); minimum ligation evolves to around 2. The bands which increase to a maximum (red, blue and yellow, brown) are the oscillating populations of the RNA pairs forming the replicase. The 2 lower bands which initial increase and then die out are the initial and mutant parasites. Notice that the latter die out when maximum ligation reaches its equilibrium value, but the average ligation strength still decreases slightly. Later sporadic evasions (white dots at the bottom) use locally occurring near above average ligating replicases. For colourfigure check www.kluweronline.com/issn/0169–6149.

The observed eco-evolutionary stability of the various models is as follows.

- *6-Membered hypercycles* are resistant to parasites in ecological time (i.e. the parasite is expelled rapidly), but destabilize in evolutionary time (see Figures 1a and b). This is because the stability properties are based on competition between the self-organized spatial patterns, here spirals. However, spiral cores are lost over evolutionary time (and only seldom recreated, Boerlijst and Hogeweg, 1995) and when only one spiral is left, this one becomes vulnerable, and eventually dies out either by parasite invasion into its core, or, more commonly due to drift of the strength of catalysis of the various molecules, which causes instability of the spiral core (see Figure 1b).
- *2-Membered hypercycle*. In contrast to long hypercycles (>5 members) which expulse parasites in ecological time, and intermediate hypercycles of 3–5 members, which are quickly destroyed, minimal hypercycles of two members, can coexist indefinitely with a strong parasite on one of its members in abcence of mutations. The system forms chaotic waves, where the parasites outcompete the hypercycle locally, but only the hypercycle can invade empty space. However, when catalytic strength evolves, the parasite is expelled in evolutionary time whatever the mutation rate is (see Figure 1c). This is because the hypercycle uses the following 'trick': the molecule which gives catalysis to the parasite does not increase the catalysis it gets itself, but the parasite and the other member of the hypercycle do increase the catalysis they get. Thus, the patches of the hypercycle become less invadable for the parasite, because they contain less catalysts for the parasite. Such patches out-compete other hypercycle patches, hence the evolutionary 'restraint' of the parasitised catalysts. The increase of catalysis of the other member of the hypercycle is faster than that of the parasite, because, unlike the parasite, it has no negative effects of getting more catalysis. Therefore, in the end the hypercycles outcompetes the parasite. However, when new parasites are created continuously, and on both members of the hypercycle, this trick renders the system very vulnerable to new parasites on the stronger member of the hypercycle and the system dies out in most cases. An interesting long term coexistence of the 2 membered hypercycle with parasites on both members can, however, occur when the continuously generated parasites are fairly mild, and the mutation rate is high; in that case no strong asymmetry is formed, and the system persists, showing long term oscillation of dominance of parasites on either member of the hypercycle (see Figure 1d).
- *Replicase and parasites*. Like the parasitised 2-membered hypercycle, one replicase and parasites can persist in ecological time, forming wave patterns. However, parasites can be only moderately strong (runs were initialized with parasite only 1.3 times as much catalysis as the replicase). In evolutionary time the outcome depends on mutation rate and chance (see Figure 2): either the parasite is expelled, or the system dies out. The latter is most common

at low mutation rates, the former at higher mutation rates, but the two modes exist as alternate attractors over a wide parameter range. As seen in Figure 2 the two modes are preceded by the slowing down of evolution toward higher catalysis in either the replicase (extinction) or the parasite. The short run effect of doing so, paradoxically, increases the average population size of the one 'giving up'. In the former case, parasite waves get stronger and stronger, the parasites almost kill themselves and their replicase, and the replicase fills up the entire field before being attacked again. In the latter case parasites do not locally outcompete the replicases completely, and the replicases then increase their diversity, and parasites cannot regain large strength toward all variants, and are outcompeted. Continuous creation of parasites destroys the system.

- RNA replicase and parasites. The models above ignore a defining feature of RNA replicators, i.e. complementary replication. Here we examine a minimal RNA model with complementary replication, in which one of the strings (e.g. the negative one) of one population is a replicase and the second pair of RNA strings represents the parasite. This model is much more persistent than either of the previous models. The surrounding of the replicase by its complementary RNA contributes much to this stability. This makes the replicase less accessible to the parasites. For lower mutation rates replicases and parasites coexist in persistent wavy patterns, which persist for a long time, but may lead in the long run (>1 million time-steps) to extinction of the system: catalysis of parasites increases somewhat faster than that of replicases. At higher mutation rates the initial parasite population is expelled. Continuous creation of parasites does not destroy the system, when we use up to 1% of the mutations leading to parasites with 5 times the maximum increase of catalysis of a normal mutant. Such parasite influx fails to destroy the system, even under the unrealistic assumption that both the plus and the minus string increase the received catalysis by that amount. In these systems parasites typically are present in a large majority, whereas the minority of replicases sustain the system (compare Hogeweg, 1994).
- *RNA duplex replicase and parasites*. In this model we assume that 2 replicators are needed to make a functional replicase. Note that in this model, unlike the previous ones, coexistence of various classes of molecules is functionally used within the system. We assume that the negative strands of two RNA molecules ligate with a certain probability when they are neighbors. In ligated form they catalyze the replication of all other RNA's (including their own type and their complements and parasites) but they themselves can not replicate. In this case our default initialization is not viable: parasites kill the system when started with a random mixture of molecules. However, when the duplex forming species are allowed to self-organize in a banded configuration (see Figure 2) before the parasites are introduced, the system survives, and in fact is extremely resilient. Unlike all previous systems parasites never gain a numerical advantage they are expelled in relatively short time, and the system

becomes non-invadable for continuously created parasites (of the type tested in the single RNA system). The following points cause this resilience.

1. If ligation is not immediately lost when parasites are created as mutants of the replicase, they very effectively destroy their own environment, and they can never invade. To study the system further ligation was set artificially to zero in the newly created parasites.
2. The spatial configuration: parasites are prone to lose the interface between the two RNA populations, and only there are duplex replicases formed; increase of catalysis of the parasite is therefore restricted.
3. Inaccessibility to duplexes is enhanced when one of the RNA duplex forming populations dominates the system; such dominance evolves.
4. Ligation probability evolves to minimal values to sustain the duplex forming species. This minimal value cannot sustain parasites which are typically located less favorably.
5. High diversity of replicases. Replicases most often replicate 'themselves' and their complements, whereas the parasites have to rely on a variety of replicases. The evolved replicase toward 'self' is higher than to others, including parasites.

When the ligation probability is free to evolve the latter two mechanisms primarily cause the extinction of the parasite population (see Figure 2). If ligation probability of the replicase subunits is fixed to a relatively high value, the other features are the primary cause of the suppression (and periodic extinction) of the continuous invading parasites.

We should note, however, that the system, unlike all other systems tested cannot survive the highest mutation rates (0.1024). This is because ligation probability is drifting to too low values, i.e. the mutation rate is above the error threshold. If ligation probability is fixed at 0.15 the system does survive with this high mutation rate, sustaining a continuous inflow of strong parasites. Note that ligation is a strong 'altruistic' trait (it prevents self-replication and promotes replication of others). The indirect selection gives a relatively low selection coefficient and therefore a lower information threshold.

Comparing the different interaction networks studied we note that the two recurring mechanisms over evolutionary time by which replicases can 'defend' themselves against co-evolving parasites are.

(1) Patch level selection causing one or more species to slow down the increase (or even decrease) the amount of catalysis which it gets, so that the patch it inhabits becomes less invadable, and
(2) Population level diversity of the replicases, so that it becomes harder for the parasite to coevolve with all of them. Their availability and their usage depends on the system architecture and other evolutionary constraints. Our experiments

suggest that complementary replication by itself protects the system from parasites, and that the more complex systems have more evolutionary leeway to enhance persistence.

3.1. Conclusion: Stable cooperation is space

The series of paradigm systems discussed above demonstrate again (like e.g. Boerlijst and Hogeweg, 1991; Hogeweg, 1994; McCaskill *et al*., 2001; Czaran and Szathmary, 2000) the lowered vulnerability of cooperative interactions to parasites in spatially extended systems. We extended the previous studies by examining long term evolution and comparing interaction architectures. This comparison shows that the complementary replication of RNA increases its eco-evolutionary potential. In the case of duplex formation, the resulting spatial structure is particular effective in 'marginalizing' parasites, once it is established.

McCaskill *et al*. (2001) studied the ecological stability of the minimal model analytically, and demonstrated its persistence in a infinite dimensional infinite size small patch model. They argued that stochastic effects, rather than spatial pattern formation are responsible for the persistence. This holds for the minimal model in ecological time. In evolutionary time 'who meets whom' becomes important, and therewith spatial separation, and the protective shield interaction partners may create.

Our experiments highlight the importance of mutation rates. By studying prior defined functional lineages, we can easily distinguish functional diversity and mutational diversity in the system. The results show that increase in diversity of the catalytic specificity in the population eliminates in evolutionary time parasitic lineages. The parasites have to cope with more diversity, and may be unable to maintain high catalytic strength relative to enough encountered interaction partners. This is an information threshold like phenomenon.

4. Vesicles and Higher Order Selection

In contrast to the previous section, in which multiple levels of selection arose automatically due to spatial pattern formation, in this section we examine what imposed new levels of selection can do for information integration in early evolution. To this end we reexamine the stochastic corrector model as first defined by Szathmary and Demeter (1987) and further studied by Grey *et al*. (1995). Our models differ from those studied earlier in this context and in the context of 'group selection' (Wilson, 1975) in the following ways:

- we study a spatial version of the model, both with respect to molecular dynamics and with respect to vesicle dynamics.
- we include vesicle dynamics instead of assuming chemostat condition (Szathmary and Demeter, 1987) or potential unlimited growth (Grey *et al*., 1995).

- in the model there is a mutual dependence of vesicle dynamics and molecular dynamics.
- we study the classical problem of the information threshold for non-catalytic self-replicating molecules (Note that the studies cited above studied catalytically interacting molecules).

Like many previous authors we simplify the molecular replicator model by distinguishing only between the master sequence (x) and all the rest (y), assuming that master sequences mutate to the rest group, but not vice versa. As elucidated by Altmeyer and McCaskill (2001), local interactions in space lower the information threshold relative to that of a well mixed system, due to limited diffusivity: the master sequence is more likely to compete with other master sequences for space due to clustering. This lowers the effective selection coefficient and therewith the information threshold, for our parameters, from an error rate of $\mu = 0.375$ in the ODE mean field model* to $\mu = 0.33$ in the corresponding full spatial model without compartments. Note that in the discrete, finite, spatial model with infinite diffusion applied in between reaction steps, the measured information threshold is identical to the ODE mean field model. Thus, not the discreteness or the local competition but the limited diffusion and pattern formation lowers the information threshold.

Moreover, it is well known that small population size lowers the information threshold as well. The finite population effect is known as Müllers Ratchet**. For recent treatments see Campos and Fontanari (1999) and Van Nimwegen and Crutchfield (2000). Compartments lower both the diffusivity and the population size. We study whether the stochastic corrector effect can over-compensate these negative effects and increase the error rate at which the master sequence can be maintained. We take the non-compartment spatial information threshold as reference.

4.1. Coupled models of replicator and vesicle dynamics

We fix the molecular level dynamics, using the following cellular automata rules.

- Reaction step: if a patch is occupied it changes its state to empty with a probability d = 0.1; if empty, it chooses one of 8 neighbors randomly; if the chosen patch is occupied the empty patch is filled with its offspring with probability $r_x = 0.8$ for master sequence and $r_y = 0.5$ for mutant sequence.
- Diffusion: 1 step of Margolus diffusion (see Toffoli and Margolus, 1987).
- Vesicle levels dynamics as described below.

* $x' = r_x q x(1 - x - y) - dx$; $y' = (r_y y + r_x(1 - q)x(1 - x - y) - dy$ with $r_x = 0.8 r_y = 0.5$; $d = 0.1$.

** Müller's ratchet is traditionally considered in the context of the evolutionary fate of finite asexual populations or non-recombining portions of the genome. However, the 'meltdown' of the population by too high mutation rates relative to the population size is the same phenomenon as the information threshold for high mutation rates in infinite population.

- Iterate.

We examine the following vesicle level selection protocols. Note that in all cases the fastest replicating molecules favor the vesicles in which they live, i.e. there is no conflict between levels of selection.

1. *Neutral model* Vesicles act as 'passive compartments', i.e. they do not 'recognize' different types of molecules. Vesicles division occurs when a certain molecular population size is reached. Because of the faster replication rates of the master sequence, the compartments add a second level of positive selection to the master sequence. This model represents the best representation for the question whether compartment alone can raise the information threshold. In other words, no new 'function' of the molecules is introduced alongside the introduction of the vesicles.
2. *Differential division model* Division of vesicles depends on the population size of the master sequence, rather than total population size. Decay of vesicles is independent of molecular content (except when empty).
3. *Linear mortality model* Decay rate of the vesicles depends linearly on the ratio of master sequence and mutant sequence. Division depends on total population size.
4. *Step mortality model* Only vesicles which have lost all master sequences decay. Division depends on total population size.

A general mean field approximation of the vesicle dynamics, distinguishing between 'good vesicles' X, which do contain master sequences ($x > 0$) and 'bad vesicles' Y (in which $x = 0$) can be written as:

$$\begin{aligned} X' &= G(x, y)Q(x)XF(X, Y) - M(x)X - D(x, y)X \\ Y' &= (gY + (1 - Q(x))X)F(X, Y) + M(x)Y - dY \end{aligned} \tag{1}$$

The maximal growth rate $G(x, y)$ of the good vesicles depends on its composition, i.e. the number of master and mutants it contains, whereas for the bad vesicles it is constant (g). The actual growth rate of all vesicles is governed by a density dependent term ($F(X, Y)$), i.e. depends on the available space. Transition rate from good vesicles to bad vesicles(maturation) depends on the number of master sequences in the good vesicle ($M(x)$), as does 'vesicle mutation rate' ($1 - Q(x)$). The decay term can again be a function of vesicle composition in the case of the good vesicles ($D(x, y)$), whereas it is a constant for bad vesicles (d).

The selection regimes described above pose the the following parameter constraints: in all models $G(x, y) > g$; in the differential division model $g = 0$; in the linear mortality model $D(x, y) = d - d * x/(x + y)$; in the step mortality model $D(x, y) = 0$; in all other cases $D(x, y) = d$.

Apart from the composition dependent functions instead of constants, this equation differs from the standard simplified replicator equation in the fact that trans-

ition from X to Y occur during the lifetime of the vesicle and not only at replication. We will refer to this process as 'maturation'.

4.2. SHIFTING THE INFORMATION THRESHOLD

An overview of the ability of the compartmentalization to shift the information threshold is given Figure 3 for each of the four selection regimes.

4.2.1. *Compartments Alone do not Increase Information Threshold*

The first column shows the parameter regions in which the information threshold of the vesicle model exceeds that of the non-compartmentalized situation. We fix the molecular dynamics, and use the mutation rate corresponding to the the information threshold in absence of vesicles ($\mu = 0.33$) and vary the two vesicle level parameters: the threshold molecular population size for vesicle division (DIVPOP) and the vesicle mortality D; note that changing these parameters has slightly different meanings in the different models. DIVPOP refers to the total population $(x + y)$ of sequences in a vesicle in all models apart from the differential division model, where it refers to only the number of master sequences x. Likewise in the step mortality model changing D affects only the bad vesicles, whereas in the other cases it affects the good vesicles as well, in the linear mortality case in a composition dependent fashion.

Parameter regions in which the master sequence persists ($x > 0$ and hence $X > 0$), only mutant sequences persist ($x = 0$; $y > 0$ and hence $X = 0$ and $Y > 0$) and extinction of all sequences ($x, y, X, Y = 0$) are indicated. All models in which the master sequence is recognized by the vesicles have a parameter regime

Figure 3. Left column: Bifurcation diagrams on vesicle level parameters, DIVPOP, the molecular population size required for vesicle division and vesicle death rate (the indicated value is the death rate of the bad vesicle, that of the good vesicles follows from the parameter constraints of the various models, as given in Section 4.1). Sequence level parameters are: replication rates $r_x = 0.8$ and $r_y = 0.5$; decay rate $d = 0.1$; and mutation rate $\mu = 0.33$, i.e. the mutation rate at the information threshold in the spatial model without vesicles. + Indicates survival of the master sequence, i.e. vesicle dynamics increases the information threshold; – indicates only mutant sequences survive and * indicates extinction of all sequences (and vesicles). Middle column: Frequency of master sequences in vesicles which do contain master sequences, against sequence mutation rate μ. For each model we show two different values of vesicle size (DIVPOP) as indicated by D = in the figure near its maximum information threshold; For each DIVPOP we show three different death rates of the vesicles: low (black), middle (red) and high (green), chosen so as to include the value for which the information threshold is maximum. See right column for the decay values used. The dotted line denotes the frequency of master sequences in the model without compartments. The X in the Neutral model indicates the information threshold in vesicles of size 80 without selection. Right column: Information threshold as function of vesicle death rate, for various values of vesicle size: Neutral model DIVPOP = 10, 40, 80; Differential division model DIVPOP = 5, 10, 15; Linear mortality model DIVPOP = 10, 20; and Step mortality model DIVPOP = 10, 40, 80. The vesicle death rates displayed in the middle column are indicated by L (low), M (middle) and H (high).
For colourfigure check www.kluweronline.com/issn/0169–6149.

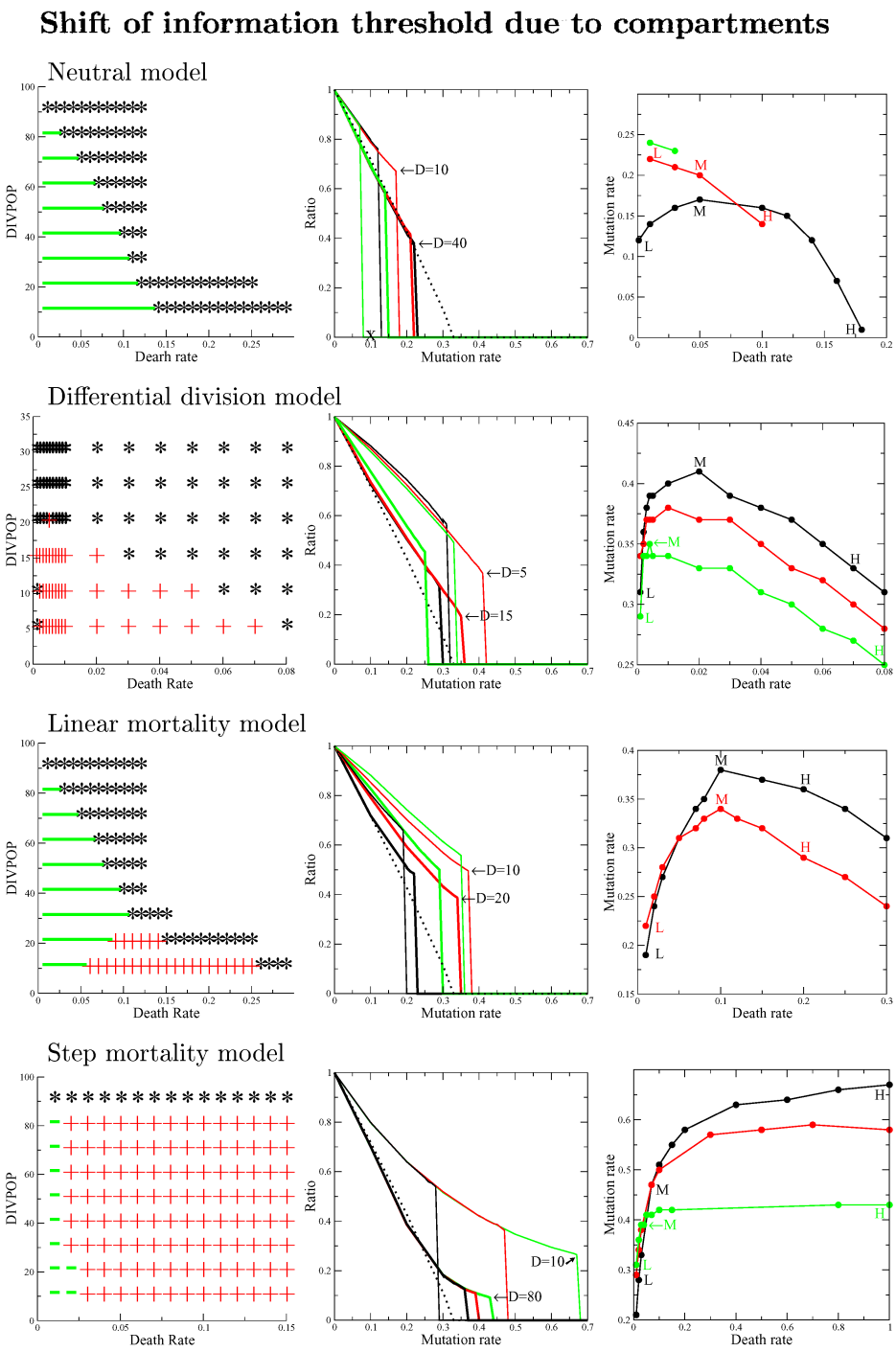
Shift of information threshold due to compartments
Neutral model
DIVPOP
Dearh rate
Ratio
←D=10
←D=40
Mutation rate
Mutation rate
Death rate
Differential division model
DIVPOP
Death Rate
Ratio
←D=5
←D=15
Mutation rate
Mutation rate
Death rate
Linear mortality model
DIVPOP
Death Rate
Ratio
←D=10
←D=20
Mutation rate
Mutation rate
Death rate
Step mortality model
DIVPOP
Death Rate
Ratio
D=10
←D=80
Mutation rate
Mutation rate
Death rate

Figure 3.

in which the master sequence persists, i.e. the vesicle level dynamics increases the information threshold. However, this is not the case for the neutral model, which either maintains a population of bad vesicles or dies out.

We conclude that an extra function which 'comes for free' is needed to make compartments a feasible scenario for increasing the amount of information maintainable in the single molecules. In other words an additional functional differentiation between the molecules is needed. This functional differentiation increases the effective selection coefficient between the master sequence and the mutants. In a certain sense the increase of the information threshold is therefore 'trivial' as the information threshold depends on the selection coefficient (compare Krakauer and Plotkin (2002) and Krakauer and Sasaki (2002)). In the linear mortality model and the step mortality model this extra selection is very direct as, together with the vesicles, mutant sequences are preferentially killed. If in the non-compartment model, mutant sequences are killed off at a similar high rate, the resulting error threshold is higher than that of the vesicle model.

4.2.2. *Vesicle Extinction Limits Information Threshold*

The second column of Figure 3 shows the traditional information threshold plots for the vesicle based models, where we plot the average ratio of master sequences maintained in 'good vesicles', against mutation rate. We show the lines for three decay rates (low, medium, high, chosen so as to include the maximum information threshold) and for two values of DIVPOP. We observe the following points:

1. in all cases there is an abrupt cutoff at a certain mutation rate. The cutoff corresponds to the extinction of the good vesicles (see Figure 6).
2. the number of master sequences in the good vesicles decreases with increased mutation rate but, in particular in case of vesicles with low values of DIVPOP, this decrease is slower than in the non-compartmentalized control.
3. at the cutoff point good vesicles are still quite good. Indeed, extrapolating the lines beyond the cutoff would yield a quite impressive improvement of the information threshold!
4. the lines for different vesicle death rates are close to each other. In the step mortality model they are strictly on top of each other, whereas in all other cases the lines are ordered according to vesicle death rate. However, only in the linear mortality model do they diverge appreciably, the highest death rates sustaining the most master sequences. In most other models the ordering is the other way around and the differences are always very small.
5. however, the information threshold, i.e. the mutation at which the cutoff occurs, clearly differs depending on vesicle death rates, as is detailed in the rightmost column of the figure.
6. as expected, vesicles which contain larger molecular populations benefit less from the vesicle dynamics, and the maximum information threshold is only slightly above the non-vesicle level.

4.2.3. *Maximum Information Threshold Depends on Rate of Vesicle Dynamics*
In the rightmost column of Figure 3 we plot the information threshold as a function of the death rate of the vesicles. We observe:

1. a maximum information threshold occurs at intermediate death rates for all models except the step mortality model, in which only vesicles without master sequences are killed.
2. at high vesicle death rates, the master sequences survive higher mutation rates in small vesicles than in larger ones.
3. however, at low vesicle death rates the reverse is true: higher mutation rates are tolerated in the larger vesicles; however, the tolerated mutation rates are relatively low for those parameters.

The reversal (item 2 and 3 above) can be seen as the 'take-over' of the vesicle dynamics, at higher vesicle death rates, over the molecular dynamics with respect to the information threshold.

In the neutral model the maximum information threshold occurs in the 'molecular regime', i.e. larger vesicles are favored, and the information threshold remains below the non-compartmental case. However, also here vesicle level selection plays a role as the information threshold is higher than without vesicle level selection: the X on the x axis represents the error threshold when vesicles divide and die randomly, using a logistic density dependent division rate.

In all other models the maximum information threshold occurs in the 'vesicle regime', and is higher than in the model without vesicles. The shape of the curves can be explained largely in terms of the vesicle level dynamics as discussed in the next section.

We conclude that the extend to which the information threshold can be shifted due to compartments is very limited because of vesicle level dynamics. As mentioned above, in order to increase the information threshold at all, the molecules with maximum replication rates, should in addition actively support the vesicle, either by increasing its survival (mortality models) or increasing (here being required for) its division. Moreover, even if we accept such a lucky coincidence, the increase in mutation threshold is only slight (<20%) except for the step mortality model with a small within-vesicle population size. In the last case vesicle level selection can increase the selection coefficient between the sequences very strongly by instantaneous death of the bad vesicles and its entire molecular content. The vesicle death rates needed to allow a 50% increase in the information threshold is equal to the molecular decay rates, which may be somewhat unreasonable in natural conditions. Nevertheless, such a selection regime might be realizable in *in vitro* selection experiments.

4.3. INTERPLAY BETWEEN MOLECULAR LEVEL AND VESICLE LEVEL DYNAMICS

In this section we discuss the mechanisms and the dynamics, which lead to the above described behavior in more detail.

4.3.1. *Vesicle Level Dynamics and the Maximum Maturation and Information Threshold*

In order to get insight how vesicle level dynamics by itself can influence the information threshold, we simplify Equation (1) by assuming fixed parameters for growth rate, death rate and quality of vesicle replication. In other words we assume that the composition of the vesicles does not change, and/or does not influence their properties. Note that this is true by definition for the death rates in all but the linear mortality model. Assuming moreover the most studied density dependent dynamics (logistic growth)* the equations can be written as:

$$\begin{aligned} X' &= g_g q X(1 - X - Y) - mX - d_g Y \\ Y' &= (g_b Y + (1 - q) g_g X)(1 - X - Y) + mX - d_b Y \end{aligned} \tag{2}$$

with g_g; g_b and d_g and d_b the growth and death rates in good and bad vasicles, and q and m the vesicle mutation and maturation rate. The parameter constraints for the different models are as indicated above (neutral model $g_g > g_b$ and $d_g = d_b$; differential division model $g_g > g_b = 0$ and $d_g = d_b$; step mortality model $g_g > g_b$ and $d_b > d_g = 0$; linear mortality model $g_g > g_b$ and $d_b > d_g$).

In analogy with the information threshold in the standard replicator equation, we can solve these equations for the maximum maturation rate (M), which can sustain good vesicles.

We plot this maximum tolerable maturation rate as a function of vesicle decay rate in Figure 4. At lower decay rates the maturation threshold depends primarily on the selection coefficient between the two types of vesicles, whereas at high decay rates it simply depends on the growth minus death rate. The overall shape of the curve is strikingly similar to that of the maximum observed (tolerated) maturation rates as shown in the lower part of the figure. The simplified model nicely predicts the occurrence and relative location of the maximum.

The limits on maturation rate in relation to growth and death rates also determines the limits on the maximum tolerable mutation rate (information threshold) in the full model. The maturation rate depends of course on both the mutation rate and the composition of the vesicles, which vary in consort in the full model. Indeed the information threshold as function of vesicle death rate has a similar shape, and in most cases the same location of the maximum, as the here depicted maturation threshold (see Figure 3).

* In spatial models a parabolic dependence is more realistic but this does not influence the qualitative argument we want to make.

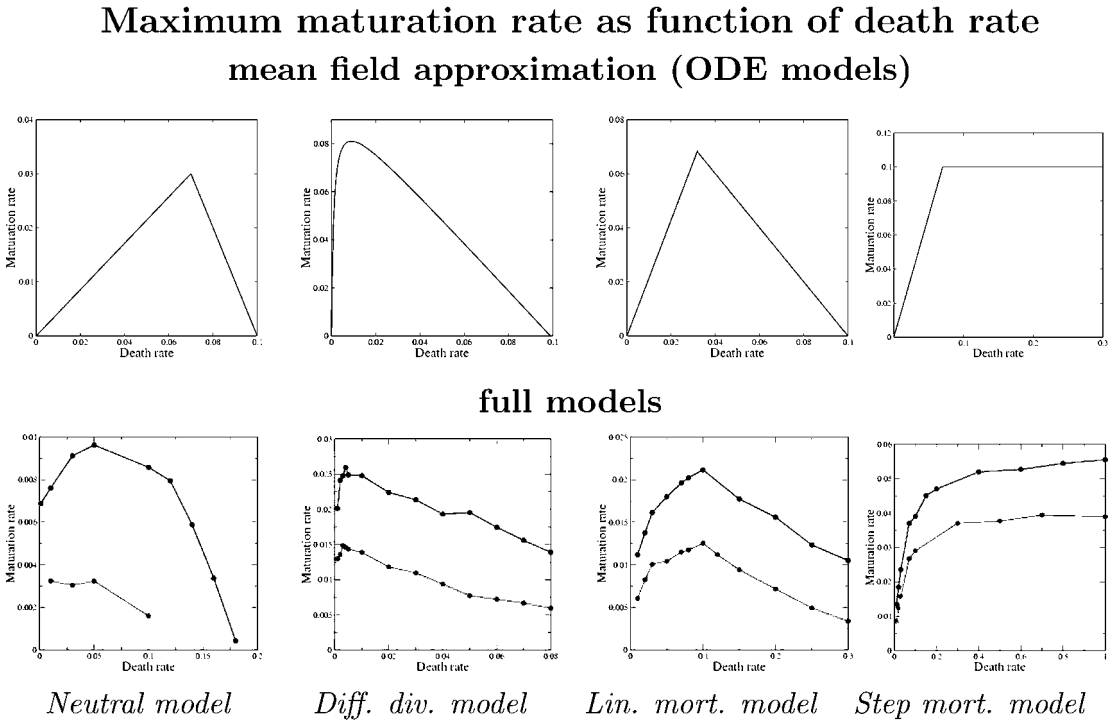

Figure 4. Based on Equation (2), and the parameter constraints for the various models the maximum tolerable maturation rates can be computed, and are given by: neutral model: $M < (G(x, y)/g - 1) * d$; and $M < G(x, y) - d$; differential division model: $M < G(x, y) * (1 - X) * d - d * d)/(G(x, y) * X + d)$; linear mortality model: $M < (a * G(x, y)/g - 1) * d$ and and $M < G(x, y) - d$; step mortality model $M < (G(x, y)/g) * d$ and $M < G(x, y)$. These functions are displayed using the following parameters: $G(x, y) = 0.1$; $g = 0.07$; $X = 0.001$; $a = 5$, where $d_{\text{bad vesicles}} = a * d_{\text{good vesicles}}$. The lower panel plots observed maximal maturation rates as function of death, linear mortality model: $M < (a * G(x, y)/g - 1) * d$ and $M < G(x, y) - d$; step mortality model $M < (G(x, y)/g) * d$ and $M < G(x, y)$. These functions are displayed using the following parameters: $G(x, y) = 0.1$; $g = 0.07$; $X = 0.001$; $a = 5$, where $d_{\text{good vesicles}} = a * d_{\text{bad vesicles}}$. The lower panel plots observed maximal maturation rates as function of death rates for different values of DIVPOP as in Figure 3.

However, unlike the simplified model the maximal growth rate of vesicles containing master sequences, depends on vesicle composition. When at higher vesicle death rates the maximum tolerable maturation rate decreases, the maximum tolerable mutation rate (information threshold) does so too. However, at lower mutation rate the vesicles contain more master sequences, which not only decreases the maturation rate, but the better composition also changes the maximum growth rate of the vesicles and therewith the allowable maturation rates. This explains the flatter peak in the information threshold plot compared to the maturation threshold plot, i.e. the lower sensitivity of the information threshold on vesicle decay rates.

For a quantitative treatment of the relation between population size, mutation rate and extinction rates (but not growth rates) see Campos and Fontanari (1999). In the next section we detail the dynamical interplay between the molecular level dynamics and the vesicles level dynamics in response to mutation rates.

4.3.2. *Changes in Vesicle Dynamics due to Mutation Rate*

The total population size of vesicles declines almost linearly with mutation rate (Figure 6). The decline of the population size of good vesicles is steeper. The extinction of the good vesicles determines the information threshold.

The molecular level dynamics percolate to the vesicle level through a change in the maximal growth rate of the good vesicles, because of a change in their composition. At higher mutation rates the quality of good vesicles deteriorates in all models, although the ratio of master and mutant molecules are kept above the non-vesicle average (see Figure 3). In equilibrium, obviously the net growth rate, the death rate and the maturation rate balance. The decrease in maximum growth rate is compensated by decrease in vesicle population size. The decrease in vesicle population size entails an increase in the size of the vesicles, which are kept below the target size through competition. Expanding vesicles create empty space for the molecules, and therefore increase in net growth rate of the molecules, and therewith increase the net growth rate of the vesicles, which depends on the size of the molecular population which it contains.

Note that the decrease in vesicle population size thus does not create 'empty space', but only increases in vesicle size over a large range of mutation rates. We see that in this way net growth rate, despite the deterioration of vesicle composition, increases to compensate for increased decay rate (linear mortality model) and increased maturation rates and increased vesicle mutation rates, which are caused by the deterioration of vesicle quality. Finally the process stops at the information threshold when the population of good vesicles dies out.

There are two different 'modes' of extinction of the good vesicles: due to competition with bad vesicles, or due to limitation of maximum growth rate. In the first case a population of bad vesicles survive, in the latter case the system goes extinct because the maximum growth rate of bad vesicles is always smaller than that of good vesicles. We discuss the neutral model and the differential division model, both with small DIVPOP in detail to demonstrate how the various processes

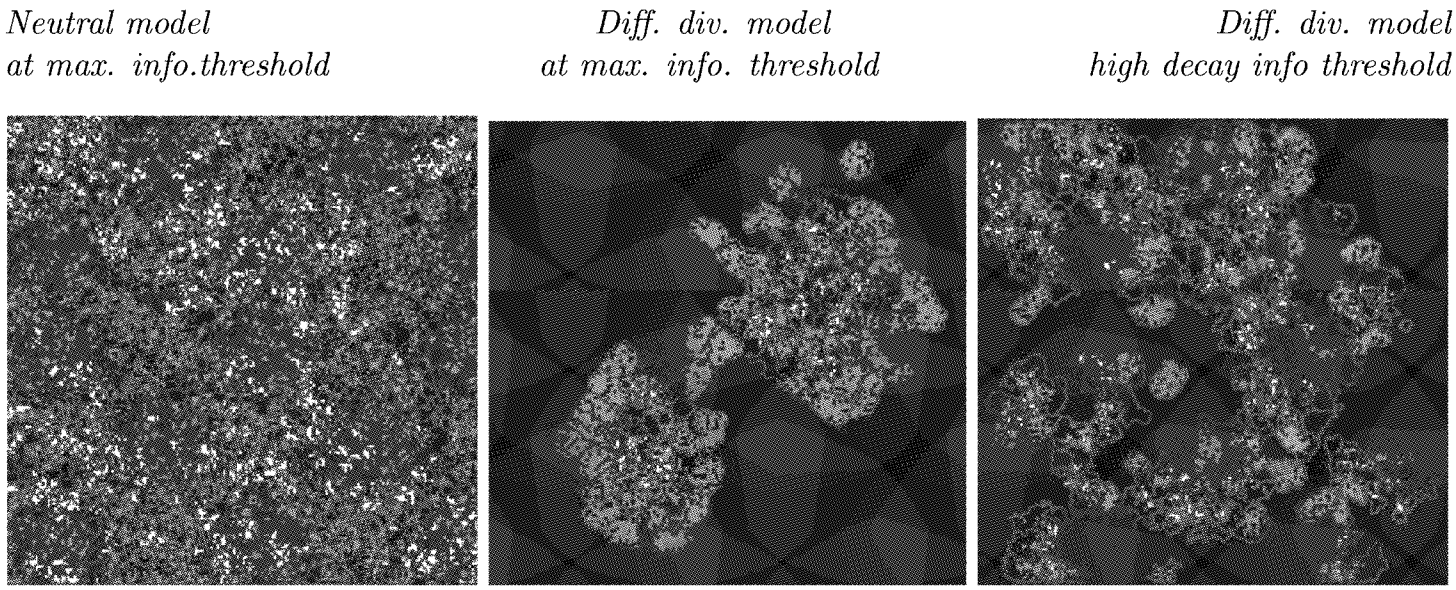

Figure 5. Spatial configuration at sequence mutation rates 0.01 below the information threshold. White dots represent master sequences, grey mutant sequences, darker gray vesicle walls. Left: Neutral model ($d = 0.05$; $\mu = 0.17$): the 'good' vesicles (containing master sequences) are outcompeted by 'bad' vesicles (without master sequences). Note the clumping of good vesicles. Middle: Differential division model ($d = 0.02$; $\mu = 0.41$): the good vesicles are surrounded by (non dividing) bad vesicle, which they create through maturation. Thus, despite much empty space net growth rate remains below maximum growth rate. Right: Differential division model ($d = 0.07$; $\mu = 0.33$): the high death rate produces a looser configuration in which vesicle competition is lower, the vesicle size is large enough relative to the molecular population size and composition to realize large net growth; the vesicles contain relatively many master sequences.

interrelate in qualitatively similar, but quantitatively different manners in different circumstances (see Figures 5 and 6.).

In the neutral model (DIVPOP=10) we note the following points.

- The maximal information threshold occurs for a vesicle death rate $D = 0.05$, for $\mu = 0.17$, i.e. far below the non-vesicle information threshold.
- We see in Figure 6 that the increase in vesicle size is limited. This is due to crowding by bad vesicles (see Figure 5).
- Therefore the deterioration of the good vesicles and the accompanying increased vesicle mutation and maturation rates, can be compensated only to a limited extent and the good vesicles die out despite their still very good quality (see Figures 3 and 5).
- In Figure 5 we see moreover, that the competitive ability of the good vesicles is also encumbered by a clustering of the good vesicles.
- At higher vesicle death rates ($D = 0.16$) much higher net vesicles growth rates can be accomplished by (very) good vesicles, while bad vesicles go extinct. In that case volume increases steeply with mutation rate.
- Because of the fast dynamics and high vesicle quality, maturation plays quantitatively no role in this case.
- However, vesicle level mutation occurs despite the high quality of the vesicles. This is because, due to the fast dynamics, molecules are more uneven distributed within the vesicle.

In conclusion, increase in information threshold by vesicle dynamics is very limited due to weak selection and spatial pattern formation.

In the differential division model with DIVPOP = 5 (master sequences) we note the following points.

- The maximal information threshold occurs for a vesicle death rate $D = 0.02$, for $\mu = 0.41$, i.e. well above the non vesicle information threshold.
- Approaching the information threshold, the volume of the vesicles peaks sharply (Figure 6).
- Because the division criterion depends on the number of master sequences in the vesicle, this number remains approximately constant for higher mutation rates, despite the decreasing ratio of master sequences: the vesicles fill up with mutant sequences, i.e. the total population at division increases with mutation rate (data not shown).
- At the maximum information threshold, despite the low total population of vesicles, and the large amounts of empty space, the growth rates of the vesicles are still limited due to vesicle competition, due to the clustering of bad vesicles around good ones, which create them at relatively high rates through both maturation and vesicle level mutation (Figure 5).

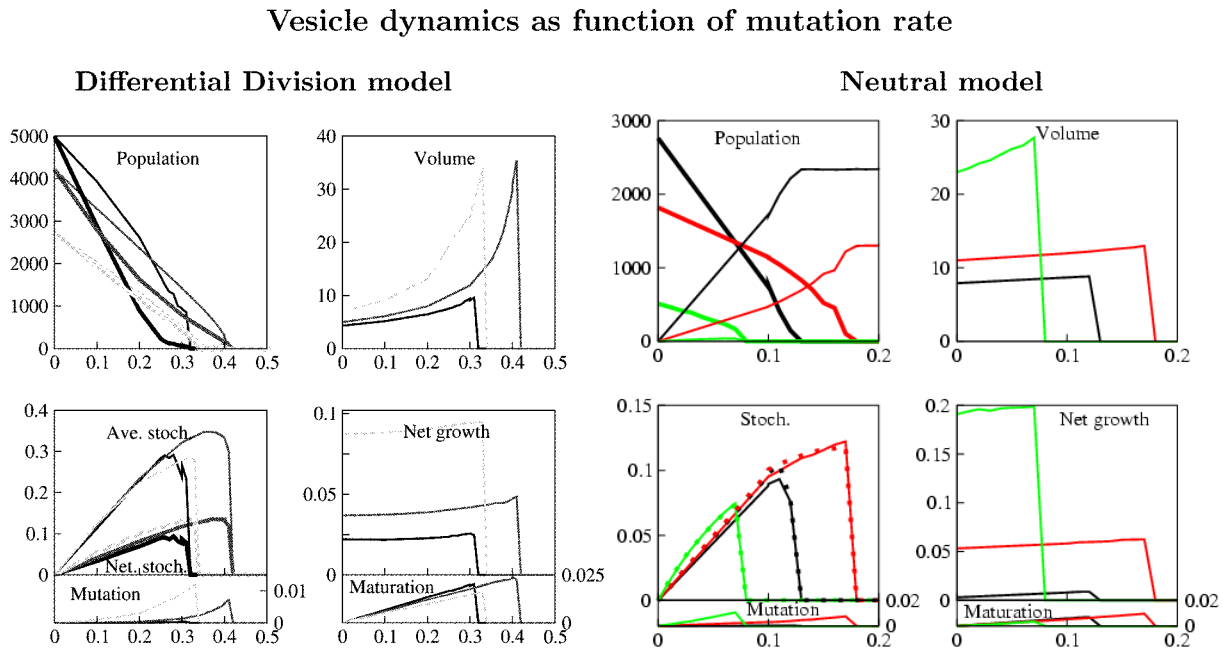

Figure 6. Various vesicle level properties are shown for the differential division model and the neutral model, for the same parameters as plotted in Figure 3, using the same color coding. The upper left pictures show the decrease of the vesicle population as function of mutation rate: total population, thin lines, and population of good vesicles, thick lines (if the lines are (almost) on top of each other, here and elsewhere dots are used). The upper right pictures show the accompanying increase in volume of the vesicles. The lower right pictures show the (slight) increase in net growth rate of the vesicles as function of molecular mutation rate, and the increase in maturation rate. The lower left pictures show the increase in the stochastic corrector effect at larger molecular mutation rates (and lower vesicle quality). The stochastic corrector effect is expressed as: $s = x_d - x_m$ (thick lines, main panel), $s = x_d - x_a$ (thin lines, main panel) and $s = 1 - q$, where x_m denotes the faction of master sequences in the mother vesicle; x_d the fraction is the best daughter vesicle and x_a the average fraction in the entire population. The vesicle level mutation rate is $G(x, y)(1 - Q(x))F(X, Y)$ (see Equation (1)) and denotes the rate of creation of a bad vesicle by the replication of a good vesicle. For colourfigure check www.kluweronline.com/issn/0169–6149.

- At higher vesicle death rates, a looser configuration (Figure 5) allows higher growth rates in vesicles with on average the same number of master sequences, but less mutant sequences, so that the molecules are packed less densely in vesicles of similar size, and can replicate faster.
- Like in the neutral model, vesicle mutation rate peaks at fast vesicle dynamics because of uneven molecule distribution (Figures 5 and 6).

The step mortality model resembles the differential division model in that bad vesicles cannot survive at the maximum information threshold (indeed they die instantaneously), while the linear mortality model resembles the neutral model in maintaining a mutant population.

In all models spatial pattern formation (clumping), both at the molecular level, and at the vesicle level influences the dynamics appreciably. It decreases effective selection at both levels, and causes high competition even at very low population levels. However, clumping of molecules also causes the vesicle mutation rate to increase sharply close to the information threshold. Note that this factor, although decreasing the survival of the good vesicles, contributes to the maintenance of good vesicles by increasing the ratio of good molecules in its sister vesicle. Thus it contributes to the 'stochastic corrector mechanism', which is the basis of all: without it, replication of good vesicles to form good vesicles beyond the (vesicles size) information threshold would be impossible.

The role of the stochastic corrector mechanism in our models is discussed in the next section.

4.3.3. *Stochastic Corrector Dynamics and Vesicle Composition*

The original stochastic corrector model as proposed by Szathmary and Demeter (1987) was based on random allocation of molecules to the daughter vesicles. In our spatial model, the daughter vesicles inherit the molecules in their 'half' of the mother vesicle. Thus the amount of asymmetric division depends not only on stochasticity but also on the spatial dynamics within the vesicles, as mentioned above. We measured the degree of 'correction', i.e. the increase of the frequency of master sequences in the vesicles by unequal division, as (1) 'net stochastic correction': the difference of the frequency of the master sequence in the best daughter vesicle and in its mother vesicle, averaged over all vesicle divisions and (2) 'average stochastic correction': the difference of the frequency of the master sequence in the best daughter vesicle and the average frequency thereof in the population of vesicles, again averages over all vesicle division event. (3) The vesicle 'mutation rate', i.e. the frequency that a bad vesicle is created by vesicle division. They are depicted in Figure 6, lower left panels for the differential division and the neutral model.

For the differential division model we note the following points.

- The net stochastic correction and the vesicle mutation increase with increased replicator mutation rate. This is to be expected because of smaller population sizes of the master sequences.
- These measures are higher for higher death rates at corresponding mutation rates This is caused by unequal distribution of the master sequences in larger vesicles, and with faster dynamics.
- In contrast the average stochastic correction is lower for faster vesicle dynamics at corresponding mutation rates, and starts to decrease close to the information threshold.
- Likewise the average quality of the good vesicles is slightly higher for slow vesicle dynamics than for fast vesicle dynamics for the case discussed here (DIVPOP = 5). This is however, not the case for larger vesicle content (DIVPOP = 15) (Figure 3)
- In all cases these differences, although slight, are consistent over all death rates indicated in Figure 3, right column.

This reversal of the influence of vesicle death rate on the average stochastic correction and vesicle quality on the one hand and the net stochastic correction on the other hand, can be understood by realizing that asymmetric division leads only to a better population average if followed up by a faster growth of the better one and/or a faster decay of the other. This 'follow up' is less for the faster death rates because of the faster dynamics: a vesicles tends to die before it matures, and growth is more dependent on opportunity (i.e. available space) than on vesicle quality. Both affect average vesicle quality, and because maturation plays a more important role for small populations of master sequences, this leads to the higher vesicle quality in the case of low values of DIVPOP, but not for higher values of DIVPOP. Decrease of composition related differential growth due to high death rates causes the reversal of the dependence on vesicle death rate of the net and the average stochastic corrector as well as the decline of the average stochastic correction close to the information threshold where net growth rate and volume effects peak.

In the other models similar effects occur: high death rates increase net stochastic correction and vesicle mutation, but decreases selection because of decreased differential growth and maturation, which affect average vesicle quality and average stochastic correction. Note, however, that vesicle growth is most closely coupled to vesicle quality in the differential division model. Therefore, in the other models average stochastic correction is similar (Neutral model, Figure 6) or below (differential mortality models) net stochastic correction. Vesicle division of below average quality good vesicles contributes relative much to net stochastic correction (as seen in the increase of net stochastic correction at higher mutation rates, cq. lower vesicle quality), but can actually decrease average stochastic correction.

We conclude that in general increased death rate has opposite effects on the asymmetric division part and the follow up part of the stochastic corrector mechanism. This can explain why the average vesicle quality is almost independent of

the death rate. Nevertheless the information threshold does depend on the vesicle death rate due to vesicle level dynamics as explained above.

4.4. Discussion and conclusions

The main conclusions of this analysis are:

- compartmentalization cannot counteract the negative effects of population size and diffusivity unless the master sequence confers an essential benefit to the vesicles. (Note that in the original formulation of the stochastic corrector model (Szathmary and Demeter, 1987) obligatory mutualistic interaction between the molecules, and therewith strong selection, were indeed assumed).
- the vesicle population dynamics largely limits the information threshold. This is not observable when chemostat conditions (Szathmary and Demeter 1987), are assumed.
- it is interesting to note that whereas the rate of vesicle dynamics has an important influence on the information threshold, it does not, or barely and in opposite direction, influence the composition of the vesicles at lower mutation rates.
- benefits of larger molecule population size in the vesicles outweigh the reduced benefits from the stochastic corrector mechanism at small rates of vesicle dynamics and/or when the vesicles confer little or no additional selection benefit beyond what is directly inherited from the molecules.
- we find that because close to the information threshold the number of master sequences is small anyhow, the stochastic corrector mechanism always does incur some benefit, also to larger vesicles.

We should note that we choose the selection regimes as extreme cases, not because of their realism, or their optimality. Indeed the performance of the model could be slightly improved by choosing an optimal division regime, or an optimal death rate regime.

It is open to discussion (or taste), whether our results mean compartments 'work' as a way to overcome the information threshold, or mean that the constraints are too severe to make it an attractive hypothesis. In particular the requirement of assuming 'function for free' is rather unsatisfactory, although multi-functionality is prevalent in biological systems. The answer depends partly on the availability of alternative hypothesis. The eco-evolutionary stability of RNA replicase based dynamics in space, discussed above provides such a potential alternative. In future work we will examine RNA replicase based version of the vesicle model to compare the performance of vesicles and large scale spatial pattern formation.

We should note that we used spatial dynamics throughout this paper. We think it is a more natural choice than well mixed systems. However, as mentioned above, doing so the reference information is lowered by ca. 10%. Note that, compared

to the information threshold in well mixed conditions, the linear mortality model as studied here does not surpass it. Note also that, as described above, spatial clumping of vesicles also has a negative effect on the extent that vesicle level selection can increase the information threshold, because it limits the growth rate of the vesicles. The mixing of the molecules within the vesicles has both positive effects by increasing the effective selection between master sequence and mutants, and better using available space, and negative effects, by decreasing the unequal division, and therewith the stochastic corrector mechanism. In the few experiments we performed the former outweigh the latter effects. Nevertheless, improvement of the internally, but not externally, mixed vesicle model relative to the mixed non vesicle model was always less than the improvement of the spatial vesicle model relative to the spatial non vesicle model.

The question of the effectives of the vesicle model in relation to the information threshold may be asked also the other way around: when vesicles arise and outcompete free living molecules (as they apparently did), do they limit the information threshold because of size and diffusivity effects?

For this question, our results show that this is not the case, provided that the selection coefficient between faster replicator molecules and slower replicating molecules is enhanced at the vesicle level.

5. Discussion and Conclusions

In this paper we discussed spatial models of prebiotic evolution. We studied the fundamental question of information accumulation through Darwinian selection. We have shown that incorporation of higher levels of selection may alleviate Eigen's paradox to a certain extend. Higher levels of selection arise automatically in spatial models in the form of spatial pattern formation. This may either help or hinder information accumulation. We have demonstrated that in particular in RNA based models spatial pattern formation of replicases and their 'dependents' can coevolve indefinite, without destruction of the replicase by being over exploited by parasites. This is in particular true in the case of duplex formation, as we have seen.

The compartment model we introduced imposes new levels of selection (the compartments) rather than generate them. The model we presented in this paper takes an intermediate position between classical models studying the compartmental benefits for information accumulation, in which the mutual interaction between the molecular level and the compartment level is limited and predefined, and more recent models which study vesicle formation as a self-organizing process of interacting replicating and hydrophobic and hydrophilic molecules (Ono and Ikegami, 2002; Breyer *et al*., 1998). This enables us to examine both a wide range of potential interactions of the levels, subject to constraints intrinsic to the fact that the dynamics of the levels are tightly coupled, as explained above. We have shown that the forces which determine inter-vesicle dynamics and intra-vesicle dynamics

are tightly interwoven. This leads to relative homestasis of some variables, e.g. the composition of the vesicles despite changing vesicle death rates, through adjustments of other variable, e.g. volume and population size of vesicles, and degree of 'stochastic correction'.

The vesicle model includes the spatial replicator model as one of its layers, and is therefore ideally suitable to compare compartments to other mechanisms of multilevel selection. We should note however, that in other aspects we have discussed evolution from quite different perspectives in the two models we presented. By studying the classical formulation of the information threshold in the vesicle model, we have assumed that there is a unique sequence which performs a certain function, here replicate itself, best. We studied not whether such a sequence will be found through evolution, but whether it can be maintained, once it has come about 'by accident'. All its mutants do perform this function as well, but less effciently.

In the spatial pattern formation model we assumed likewise that all offspring of a certain population could perform a similar function, but considered improvements of the function as well. Thus we studied a phenotypic rather than a genotypic information threshold (Huynen *et al*., 1996). We incorporated an unlimited number of different variants, instead of assuming an average population of mutants. Indeed, the ensuing diversity of the populations proved a determining factor for the eco-evolutionary stability of the interaction structures studied. In this context a process akin to the information threshold gets an other image, as by limiting the effciency of the parasite populations, it can maintain a viable system.

In future work we will further study information accumulation in vesicle based models. We need to look at interacting molecules – using similar interaction structures as those studied in non-vesicle based systems in this paper, and indeed as those studied in the initial formulation of the stochastic corrector model. The aim will be to look at information accumulation from a truly multilevel perspective, the central question being how information/diversity at different levels interrelate.

References

Altmeyer, S. and McCaskill, J. S.: 2001, Error Threshold for Spatially Resolved Evolution in the Quasispecies Model, *Phys. Rev. Lett.* **86**(25), 5819−5822.

Boerlijst, M. A. and Hogeweg, P.: 1991, Spiral Wave Structure in Pre-biotic Evolution: Hypercycles Stable against Parasites, *Physica D* **48**, 17−28.

Boerlijst, M. A. and Hogeweg, P.: 1991, 'Selfstructuring and Selection: Spiral Waves as a Substrate for Prebiotic Evolution', in C. G. Langton (ed.), *Artificial Life II. SFI Studies in the Sciences of Complexity*, Vol. X, Addison Wesley, pp. 255−276.

Boerlijst, M. A. and Hogeweg, P.: 1995, Spatial Gradients Enhance Persistence of Hypercycles, *Physica D* **88**, 29−39.

Breyer, J., Ackermann, J. and McCaskill, J.: 1998, Evolving Reaction-diffusion Ecosystems with Self-assembling Structures in Thin Films, *Artif. Life.* **4**(1), 25−40.

Campos, P. R. A. and Fontanari, J. F.: 1999, Finite-size Scaling of the Error Threshold Transition in Finite Populations, *J. Phys. A.* **32**, L1−L7.

Couwenberg, J.: 1997, 'The Fate of Cheaters on Ecological and Evolutionary Timescales', *Master's Thesis*, Dep. Theor. Biol./Bioinformatics, Utrecht.

Czaran, T. and Szathmary, E.: 2000, 'Coexistence of Replicators in Prebiotic Evolution', in U. Dieckmann, R. Law and J. A. J. Metz (eds), *The Geometry of Ecological Interactions: Simplifying Spatial Complexity*, IIASA and Cambridge University Press, pp. 116−134.

Eigen, M., McCaskill, J. and Schuster, P.: 1989, The Molecular Quasispecies, *Adv. Chem. Phys.* **75**, 149−263.

Eigen, M. and Schuster, P.: 1979, *The Hypercycle: A Principle of Natural Selforganisation*, Springer, Berlin 92 pp. (also publised in *Die Naturwiszenschaften*, 1977:11, 1978:1 and 1978:7).

Fuchslin, R. M. and McCaskill, J. S.: 2001, Evolutionary Self-organization of Cell-free Genetic Coding, *Proc. Natl. Acad. Sci. U.S.A.* **98**(16), 9185−9190.

Glazier, J. A. and Graner, F.: 1993, Simulation of the Differential Driven Rearrangement of Biological Cells, *Phys. Rev. E* **47**, 2128−2154.

Grey, D., Hutson, V. and Szathmary, E.: 1995, A Re-examination of the Stochastic Corrector Model, *Proc. R. Soc. Lond. B.* **262**, 29−35.

Hogeweg, P.: 1994, Multilevel Evolution: Replicators and the Evolution of Diversity, *Physica D* **75**, 275−291.

Hogeweg, P.: 2002, 'Multilevel Processes in Evolution and Development: Computational Models and Biological Insights', in Michael Lässig and Angelo Valleriani (eds), *Biological Evolution and Statistical Physics*, Springer-Verlag.

Huynen, M. A., Stadler, P. F. and Fontana, W.: 1996, Smoothness within Ruggedness: The Role of Neutrality in Adaptation, *Proc. Natl. Acad. Sci. U.S.A.* **93**(1), 397–401.

Krakauer, D. C. and Plotkin, J. B.: 2002, Redundancy, Antiredundancy, and the Robustness of Genomes, *Proc. Natl. Acad. Sci. U.S.A.* **99**(3), 1405–1409 (applied to prebiotic evolution in Krakauer, D. C. and Sasaki, A., Noisy clues to the origin of life, in prep.)

Maynard Smith, J. and Szathmáry, E.: 1995, *The Major Transitions in Evolution*, Freeman, Oxford.

Maynard Smith, J.: 1979, Hypercycles and the Origin of Life, *Nature* **20**, 445−446.

McCaskill, J. S., Fuchslin, R. M. and Altmeyer, S.: 2001, The Stochastic Evolution of Catalysts in Spatially Resolved Molecular Systems, *Biol. Chem.* **382**(9), 1343−1363.

Van Nimwegen, E. and Crutchfield, J. P.: 2000, Metastable Evolutionary Dynamics: Crossing Fitness Barriers or Escaping via Neutral Paths? *Bull. Math. Biol.* **62**(5), 799−848.

Ono, N. and Ikegami, T.: 2002, Selection of Catalysts through Cellular Reproduction in Artificial Life VIII. Standish, Abbass, Bedau (eds.) (MIT Press) 2002, pp. 57–64.

Szathmary, E. and Demeter, L.: 1987, Group Selection of Early Replicators and the Origin of Life, *J. Theor. Biol.* **128**(4), 463−486.

Toffoli, T. and Margolus, N.: 1987, *Cellular Automata Machines*, MIT Press, Cambridge, London.

Wilson, D. S.: 1975, The Theory of Group Selection, *Proc. Nat. Acad. Sci. U.S.A.* **72**, 143−146.